AFGL-TR-84-0151

NONLINEAR ELECTROMAGNETIC SCATTERING
FROM A DIODE CIRCUIT

Robert R. Beland

Rio Grande Associates
One Allen Center, Suite 1000
Houston, Texas 77002

Scientific Report No. 3

DTIC
ELECTE
JUL 26 1985
S
D
B

January 1984

Approved for public release; distribution unlimited

85 07 15 316

This report has been reviewed by the ESD Public Affairs Office (PA) and is releasable to the National Technical Information Service (NTIS).

This technical report has been reviewed and is approved for publication.

PAUL TSIPOURAS
Contract Manager

PAUL TSIPOURAS, Chief
Analysis & Techniques Branch
Information Resources Management Division

FOR THE COMMANDER

EUNICE C. CRONIN, Director
Information Resources Management Division

Qualified requestors may obtain additional copies from the Defense Technical Information Center. All others should apply to the National Technical Information Service.

If your address has changed, or if you wish to be removed from the mailing list, or if the addressee is no longer employed by your organization, please notify AFGL/DAA, Hanscom AFB, MA 01731. This will assist us in maintaining a current mailing list.

Do not return copies of this report unless contractual obligations or notices on a specific document requires that it be returned.

REPORT DOCUMENTATION PAGE	READ INSTRUCTIONS BEFORE COMPLETING FORM

1. REPORT NUMBER	2. GOVT ACCESSION NO.	3. RECIPIENT'S CATALOG NUMBER
AFGL-TR-84-0151	AD-A157 216	

4. TITLE *(and Subtitle)*	5. TYPE OF REPORT & PERIOD COVERED
NONLINEAR ELECTROMAGNETIC SCATTERING FROM A DIODE CIRCUIT	Scientific Report No. 3
	6. PERFORMING ORG. REPORT NUMBER

7. AUTHOR(s)	8. CONTRACT OR GRANT NUMBER(s)
Robert R. Beland	F19628-81-C-0128

9. PERFORMING ORGANIZATION NAME AND ADDRESS	10. PROGRAM ELEMENT, PROJECT, TASK AREA & WORK UNIT NUMBERS
Rio Grande Associates One Allen Center, Suite 1000 Houston, TX 77002	62101F 9993XXXX

11. CONTROLLING OFFICE NAME AND ADDRESS	12. REPORT DATE
Air Force Geophysics Laboratory Hanscom AFB, MA 01731 Monitor: Paul Tsipouras/RMA	January 1984
	13. NUMBER OF PAGES
	40

14. MONITORING AGENCY NAME & ADDRESS*(if different from Controlling Office)*	15. SECURITY CLASS. *(of this report)*
	Unclassified
	15a. DECLASSIFICATION/DOWNGRADING SCHEDULE

16. DISTRIBUTION STATEMENT *(of this Report)*

Approved for public release; distribution unlimited.

17. DISTRIBUTION STATEMENT *(of the abstract entered in Block 20, if different from Report)*

18. SUPPLEMENTARY NOTES

19. KEY WORDS *(Continue on reverse side if necessary and identify by block number)*

electromagnetic scattering: nonlinear scattering:
Volterra series: diode circuit:

20. ABSTRACT *(Continue on reverse side if necessary and identify by block number)*

Electromagnetic scattering from an active diode circuit is considered. The focus is on the nonlinear interaction between the incident fields and the internal circuit sources. This interaction results in a mixing of frequencies between the incident and internal sources. An equivalent circuit model of the diode circuit and dipole antenna is presented and a nonlinear differential equation derived. This equation is solved approximately by a Volterra series to third order. This solution is simulated and numerical values of total scattered power at the various frequencies are calculated.

DD FORM 1473
1 JAN 73

TABLE OF CONTENTS

Page

ACKNOWLEDGEMENT

DTIC
SELECTED
JUL 26 1985
B

Accession For	
NTIS GRA&I	✓
DTIC TAB	☐
Unannounced	☐
Justification	
By	
Distribution/	
Availability Codes	
Dist	Avail and/or Special
A-1	

LIST OF FIGURES

LIST OF TABLES

NONLINEAR ELECTROMAGNETIC SCATTERING FROM A DIODE CIRCUIT

I.   INTRODUCTION

The problem we treat is that of the electromagnetic scattering by a diode circuit. This is an inherently nonlinear problem: indeed, it is the nonlinear effects that are of interest. Previous authors (Franceschetti and Pinto, 1980, Landt et al., 1983, Liu and Tesche, 1976, Kanda, 1980, Sarkar and Weiner, 1976) have focused on scattering by a nonlinearly loaded antenna. This effort extends this previous work by considering the scattering from an active circuit. The focus here is on the interaction between the incident fields and the fields due to the sources in the circuit. This interaction results in a mixing of the frequency components of the incident fields and the internal source, an effect characteristic of the nonlinearity.

Our approach uses the Volterra series method for approximating the solution of a nonlinear differential equation (Sarkar and Weiner, 1976, Graham and Ehrman, 1973, Schetzen, 1980). The series solution is truncated at the third order. It is thus a perturbation method, where the nonlinear effects are regarded as corrections to the more dominant linearities. Our solution is strictly applicable to the mildly nonlinear case, but it also sheds light on the behavior of the more general case.

II. FORMULATION

We will now formulate the circuit model and derive the differential equation. The circuit we treat is shown in Figure 1. The circuit has a sinusoidal voltage source $v(t)$, a pure load resistance R_L and a diode. The antenna is a simple dipole and generates an additional voltage in the circuit due to reception of some incident RF signal. We will focus mainly on the calculation of the total scattered power at various frequencies and the voltage across the diode.

Following Kanda (1980), we will approximate the diode by a linear capacitor C and a nonlinear resistance R in parallel. The current through this resistor obeys the characteristic diode relation:

$$i_d(t) = i_s(e^{\alpha v_d} - 1) \tag{1}$$

where i_s is the saturation current and is a constant depending on temperature and v_d is the voltage across the diode. Following Liu and Tesche (1976), we will represent the antenna by its Norton equivalent circuit, i.e., by a current source, $i_{sc}(t)$ and an admittance Y_{in} in parallel (where $i_{sc}(t)$ is the short circuit antenna current and Y_{in} the antenna input admittance). We thus arrive at the equivalent circuit depicted in Figure 2.

Using Kirchoff's current law at the 3 nodes results in the differential equation

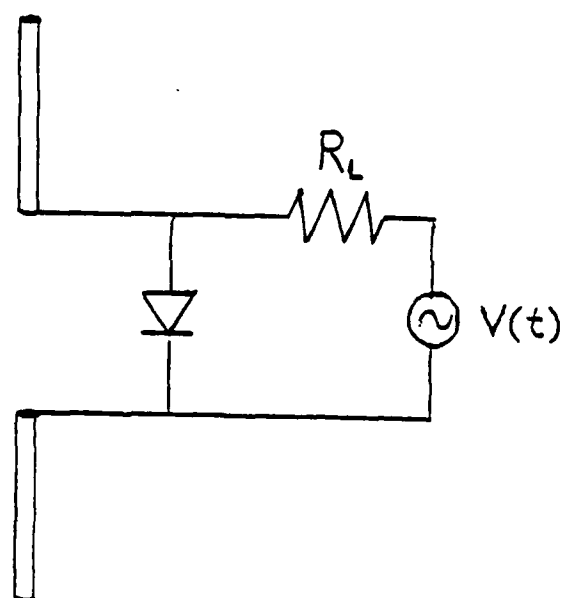$$i_R(t) = i_{sc}(t) + v(t)/R_L - [1/R_L + Y(D) + CD] v_d(t) \tag{2}$$

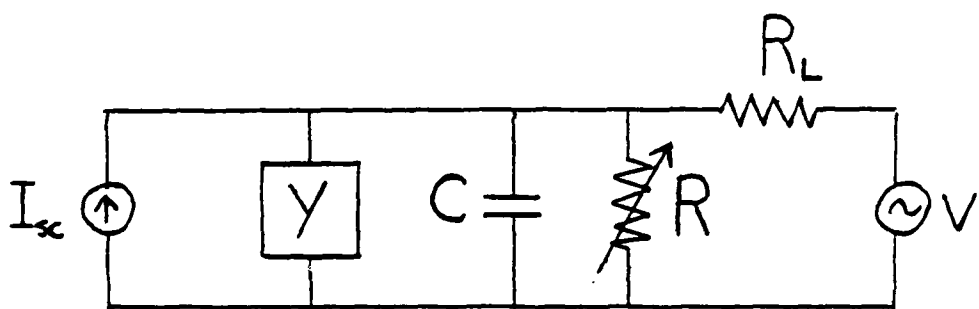Figure 1: Diode circuit with dipole antenna.

Figure 2. Equivalent Circuit Model.

where i_R is the current through the nonlinear resistor, D is the differential operator d/dt and Y(D) is a linear differential operator due to the antenna admittance. Substituting from (1) produces

$$i_s(e^{\alpha v_d}-1) = i_{sc}+ v/R_L - [1/R_L+CD+Y(D)] v_d \qquad (3)$$

This is the equation we seek to solve: the solution will yield $v_d(t)$ in terms of the driving term $(i_{sc}(t)+v(t)/R_L)$. The nonlinearity of the equation is due to the exponent. A similar, but simpler equation is treated by Kanda (ibid). The nonlinearity can be transformed into a form which is more useful for our method of solution by using the series expansion of the exponent:

$$e^{\alpha v_d} = \sum_{n=0}^{\infty} \frac{(\alpha v_d)^n}{n!} \qquad (4)$$

Substitution of this into the differential equation yields after rearrangemment of terms:

$$(i_{sc}+v/R_L) = (i_s\alpha+1/R_L)v_D + C\frac{dv}{dt} + Y(D)v_d + i_s\frac{\alpha^2 v^2}{2} + i_s\frac{\alpha^3 v^3}{6} \qquad (5)$$
$$+ \ldots$$

In this form, the driving term is apparent, as well as the linear and nonlinear parts of the equation.

III. VOLTERRA SERIES SOLUTION:

We will now use the Volterra series method (Sarkar and Weiner, 1976, Graham and Ehrman, 1973, Schetzen, 1980) to derive an approximate solution to (5). The method will utilize a series of third order and requires the approximation of the diode characteristic equation:

$$(e^{\alpha v} - 1) \cong \alpha v + \frac{\alpha^2 v^2}{2} + \frac{\alpha^3 v^3}{6} \tag{6}$$

Clearly this approximation of i by a cubic is best in the vicinity of $v = 0$, i.e., when

$$|\alpha v| \ll 1 \tag{7}$$

At room temperature, is of the order of 38 (volts) , so our solution will be strictly applicable for the domain

$$|v| \ll 0.026 \text{ volts} \tag{8}$$

To simplify the following, let us write the approximation to (5) as:

$$Y(D)[v(t)] + CD[v(t)] + (a_1 + 1/R_L)v(t) + a_2 v^2(t) + a_3 v^3(t) \tag{9}$$
$$= g(t)$$

where we have dropped the subscript on $v(t)$, the driving term is written as $g(t)(=i_{sc} + v/R_L)$ and the diode expansion coefficients are $a_1 = i_s \alpha$, $a_2 = i_s \alpha^2/2$ and $a_3 = i_s \alpha^3/6$. The Volterra series expansion for $v(t)$ to third order is:

$$v(t) = v_1(t) + v_2(t) + v_3(t) \tag{10}$$

where

$$v_1(t) = \int h_1(\tau_1)g(t-\tau_1)d\tau_1 \tag{11}$$

$$v_2(t) = \iint h_2(\tau_1,\tau_2)g(t-\tau_1)g(t-\tau_2)d\tau_1 d\tau_2$$

$$v_3(t) = \iiint h_3(\tau_1,\tau_2,\tau_3)g(t-\tau_1)g(t-\tau_2)g(t-\tau_3)d\tau_1 d\tau_2 d\tau_3$$

where all integrals are over the range $(-\infty, \infty)$ and where $h_p(\tau_1 \ldots \tau_p)$ is the pth order impulse response due to the pth order nonlinearity. Thus, $v_1(t)$ is the linear part of the response, $v_2(t)$ is the quadratic and $v_3(t)$ is the cubic. Instead of impulse responses, we may write $v_p(t)$ in terms of transfer functions:

$$v_1(t) = 1/2\pi \int H_1(w)G(w)e^{jwt}dw \tag{12}$$

$$v_2(t) = 1/(2\pi)^2 \iint H_2(w_1,w_2)G(w_1)G(w_2)e^{j(w_1+w_2)t}dw_1 dw_2$$

$$v_3(t) = 1/(2\pi)^3 \iiint H_3(w_1,w_2,w_3)G(w_1)G(w_2)G(w_3)e^{j(w_1+w_2+w_3)t}dw_1 dw_2 dw_3$$

Now, let $g(t)$ be a sum of sinusoids:

$$g(t) = \sum_{i=1}^{n} g_i e^{jw_i t} \tag{13}$$

Then

$$G(w) = 2\pi \sum_{i=1}^{n} g_i \delta(w-w_i) \tag{14}$$

It can be shown that the transfer functions are invariant under a permutation of frequencies (Schetzen, 1980). Using this property, substitution of (14) into (12) yields

$$v_1(t) = \sum_i H_1(w_i)e^{jw_i t} \tag{15}$$

$$v_2(t) = \sum_i g_i^2 H_2(w_i, w_i)e^{j2w_i t} + \sum_i \sum_{\substack{j \\ i \neq j}} g_i\, g_j\, H_2(w_i, w_j)e^{j(w_i+w_j)t}$$

$$v_3(t) = \sum_i g_i^3 H_3(w_i, w_i, w_i)e^{j3w_i t} + 3 \sum_i \sum_{\substack{j \\ i \neq j}} g_i^2 g_j\, H_3(w_i, w_i, w_j)e^{j(2w_i+w_j)t} +$$

$$\sum_i \sum_j \sum_{\substack{k \\ i \neq j \neq k}} g_i\, g_j\, g_k\, H_3(w_i, w_j, w_k)e^{j(w_i+w_j+w_k)t}$$

14

where all sums are from 1 to n. The solution of our differential equation (9) has thus been reduced to determining the transfer functions. This is straightforward but algebraically tedious and will only be outlined here (see, e.g., Sarkar and Weiner, 1976, Graham and Ehrman, 1973, Franceschetti and Pinto, 1980). Using (10) in (9) produces

$$\left[Y(D)+CD+a_1+1/R_L\right](v_1+v_2+v_3) = g(t)-a_2(v_1+v_2+v_3)^2-a_3(v_1+v_2+v_3)^3 \qquad (16)$$

With the assumption of (13), i.e., that the driving term is a sum of sinusoids, (16) can be solved. First we expand the square and cube in (16) and then substitute for v_1, v_2 and v_3, using (15) and for $g(t)$ using (13). Now the effect of the differential operators on e^{jwt} is carried out. Terms are grouped by frequency and order and equated to zero. Thus, equating terms in e^{jwt} yields the first order transfer function:

$$H_1(w) = \frac{1}{Y(w)+jwC+a_1+1/R_L} \qquad (17)$$

Grouping the terms in $e^{j(w_i+w_j)t}$ produces

$$H_2(w_i,w_j) = -a_2 H_1(w_i) H_1(w_j) H_1(w_i+w_j) \qquad (18)$$

Grouping the terms in $e^{j(w_i+w_j+w_k)t}$ and using (17) and (18) produces

$$H_3(w_i,w_j,w_k) = H(w_i+w_j+w_k)H(w_i)H(w_j)H(w_k) \times$$
$$\left\{2/3a_2^2\left[H(w_j+w_k)+H(w_i+w_k)H(w_i+w_j)\right]-a_3\right\} \qquad (19)$$

This outline of the derivation of (18) and (19) has implicitly used the property that the pth order transfer function depends only on transfer functions of lower order. Equations (17), (18) and (19), together with (15), represent the formal solution to our equation. The presence of harmonics as well as mixed frequency components is demonstrated by the expressions in (15). The magnitude of these components can be calculated from (17), (18) and (19).

15

IV. SIMULATION:

We will now use the derived solution to simulate the behavior of the circuit depicted in Figure 1. To do so, we must specify the antenna characterics, more specifically, $Y(w)$ and $i_{sc}(t)$. We will restrict ourselves to the case where plane waves are incident broadside to the antenna. This simplifies the calculation of received current considerably without obscuring the physics of the Volterra series solution. For broadside incidence of a plane wave of frequency w and amplitude E_0 on a dipole antenna, we have (Jordan and Balmain, 1968):

$$i_{sc}(w) = \frac{V_{oc}(w)}{Z(w)} = \frac{-E_0 L_{eff}}{Z(w)} \tag{20}$$

where the effective length, L_{eff}, is given by

$$L_{eff} = \frac{2(1 - \cos K\ell)}{K \sin K\ell} \tag{21}$$

where $K = 2\pi/\lambda = w/c$. The calculation of the antenna impedance (or its reciprocal, the admittance) is complicated by the frequency range of interest: we desire frequencies well below , as well as above, resonance. The method adopted uses two different methods of calculaltion. For wavelengths greater than 20 times the antenna half-length ℓ , we use the short dipole approximation (Tai, 1961):

$$Z(w) = 20 K^2 \ell^2 - j\, 120/K\ell\, [\ell n(2\ell/a)-1] \tag{22}$$

where (a) is the antenna radius. For wavelengths shorter than 20ℓ, we use Schelkunoff's method (Jordan and Balmain, ibid):

$$Z(w) = Z_0 \left[\frac{R \sin K\ell + j(X-N) \sin K\ell - (Z_0-M) \cos K\ell}{(Z_0+M) \sin K\ell + (X+N) \cos K\ell - jR \cos K\ell} \right] \tag{23}$$

where $Z_0 = 120\left[\ln(2\ell/a)-1\right]$

$M = 60\left[\ln(2k\ell)-Ci(2k\ell)+\gamma-1+\cos(2k\ell)\right]$

$N = 60\left[Si(2k\ell)-\sin(2k\ell)\right]$

$R = 60\left[\gamma+\ln(2k\ell)-Ci(2k\ell)\right]$
$\qquad + 30\left[\gamma+\ln(k\ell)-2Ci(2k\ell)+Ci(4k\ell)\right]\cos(2k\ell)$
$\qquad + 30\left[Si(4k\ell)-2Si(2k\ell)\right]\sin(2k\ell)$

$X = 60Si(2k\ell) + 30[Ci(4k\ell)-\ln(k\ell)-\gamma]\sin(2k\ell)$
$\qquad - 30Si(4k\ell)\cos(2k\ell)$

and where γ is Euler's constant and $Si(x)$ and $Ci(x)$ are the sine and cosine integrals respectively:

$\gamma = 0.5772157$

$Si(x) = \int_0^x \frac{\sin v}{v}dv$

$Ci(x) = -\int_x^\infty \frac{\cos v}{v}dv$

The use of Schelkunoff's expressions is motivated by the desire to have the impedance not only at the half-wave and full-wave resonances, but also at higher resonances. In this simulation, we will use the following values:

$\ell = 16cm$

$a = 1.6mm$

In Figure 3, the antenna impedance, using these values, is shown for frequency range 1 KHz to 1 GHz. The numerical data from which the figures were constructed showed that the half-wave resonance occurs at approximately 450 MHz and the full-wave resonance at about 820 MHz, i.e., when $Im(Z) = 0$.

The calculation of the total scattered power at frequency w is easily done if the voltage across the diode is known. From Figure 2, it is apparent the voltage across the antenna admittance is the same as across the diode. Hence, we have for total scattered power

$$P(w) = \left|i_a(w)\right|^2 R_a(w)$$
$$= \left|v_D(w)Y(w)\right|^2 R_a(w)$$
$$= \left|v_D(w)/Z(w)\right|^2 R_a(w \qquad (24)$$
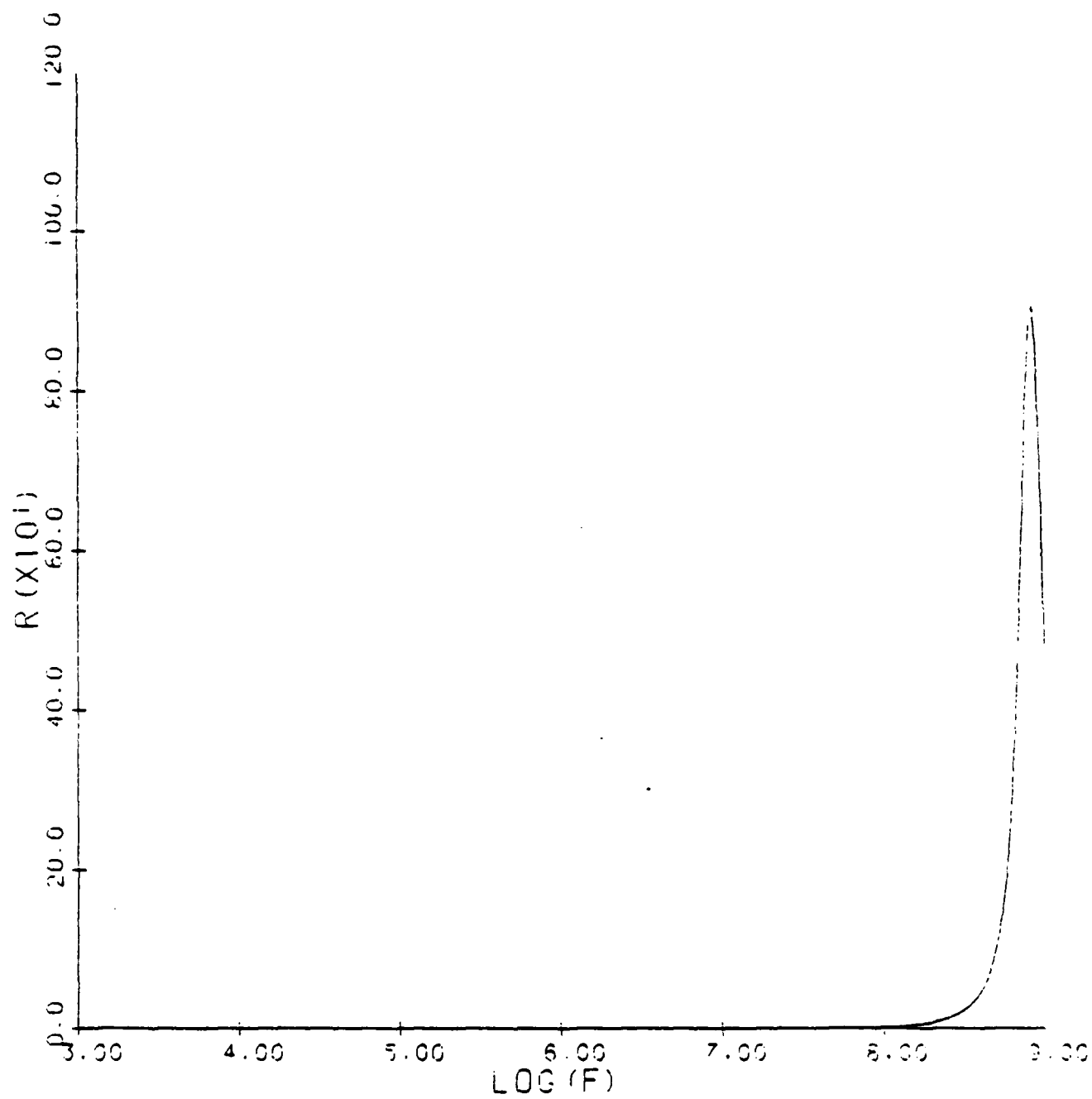
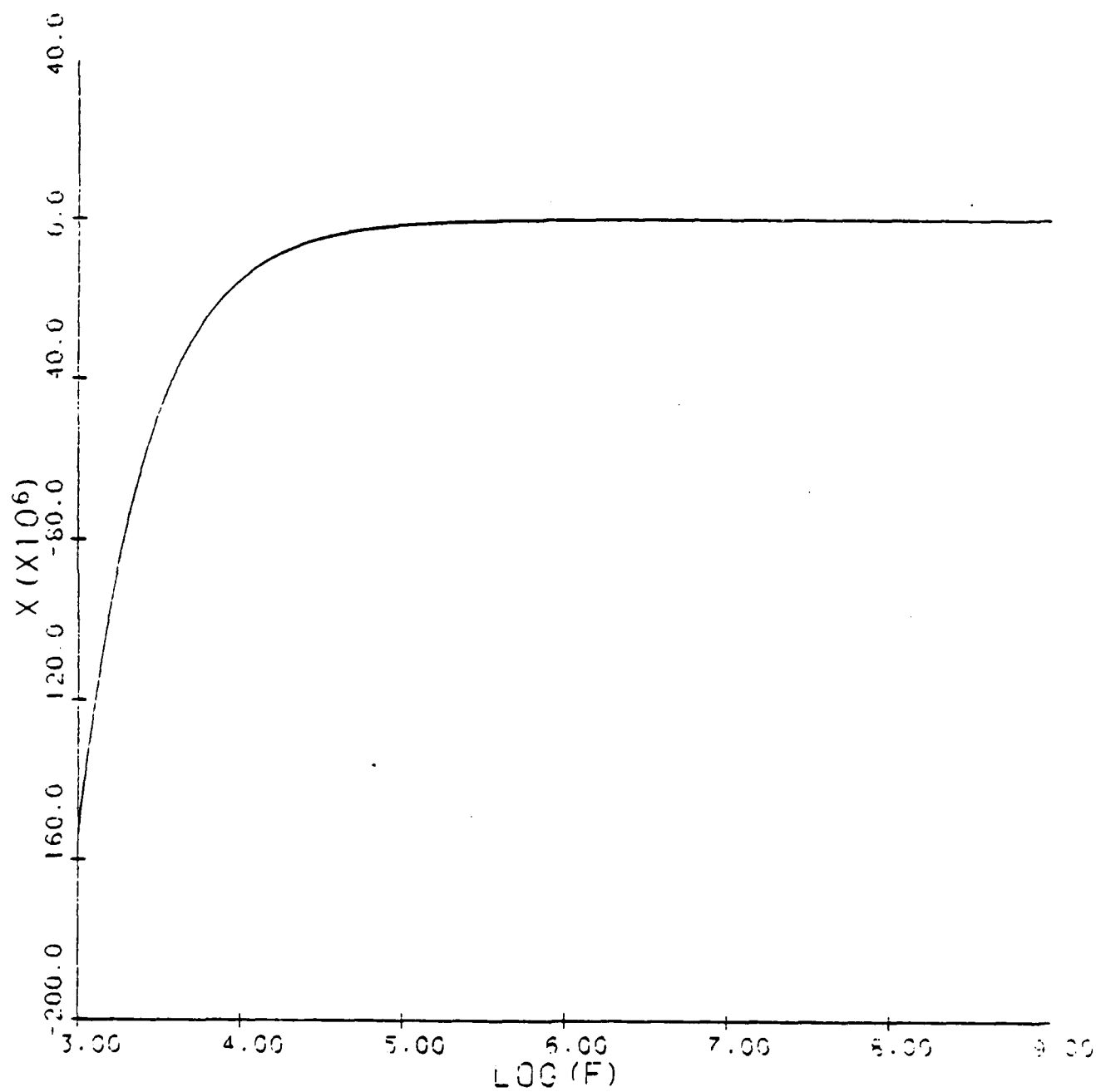Figure 3. Antenna Impedance.   a) Resistance

18

Figure 3.   Antenna Impedance.   b)   Reactance.

where R_a is the antenna radiation resistance, given by the real part of the antenna impedance $Z(w)$.

Now from equations (15), it is apparent that the characteristic behavior of the circuit is contained in the transfer functions. For this reason, we have calculated the first, second and third order transfer functions. The value of the diode capacitance C was chosen, as by Kanda (1980) to be 10^{-11} f. The saturation current was also selected as in Kanda to be 2×10^{-9} amp. The diode exponent was calculated from

$$\alpha = n/qkT$$

where the diode ideality factor n was 1, T the temperature was 20° C (293.15° K) and q and k are the electronic charge and Boltzmann's constant respectively. In Figure 4, we display the result of the calculation of the first order transfer function from equation (17), and the scattered power from equation (24). The power is not the total power at that frequency, but rather what the power would be if all other transfer functions were zero; in (24), we use $v_1(w)$ instead of v_D. The numerical data showed that the first order transfer function exhibited a maximum in modulus at 525 MHz and a maximum of radiated power at about 550 MHz.

For higher order transfer functions, there is a representational problem that accompanies the display of multidimensional data. To simplify the presentation of the second order transfer function $H_2(w_1, w_2)$, we will assume that one of frequencies is fixed at the value of $2\pi \times 20$ KHz; this audio frequency is chosen since it will be used as the frequency of circuit-applied-voltage source in what follows. In Figure 5, we present the second order transfer function $H_2(w_1, w_2)$ with w_1 fixed and the power radiated due to
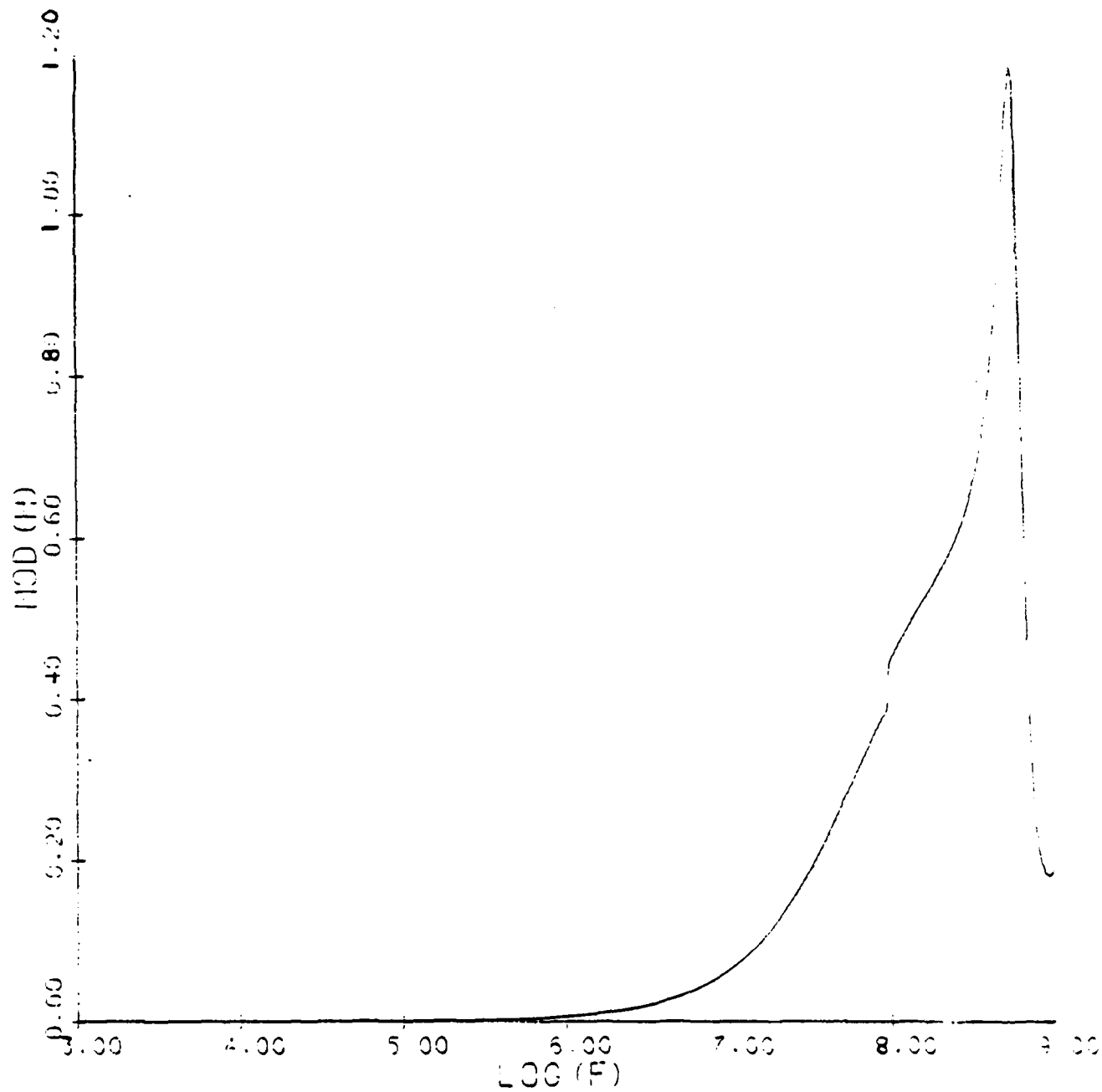
Figure 4. First order transfer function and contribution to
radiated power.   a) magnitude
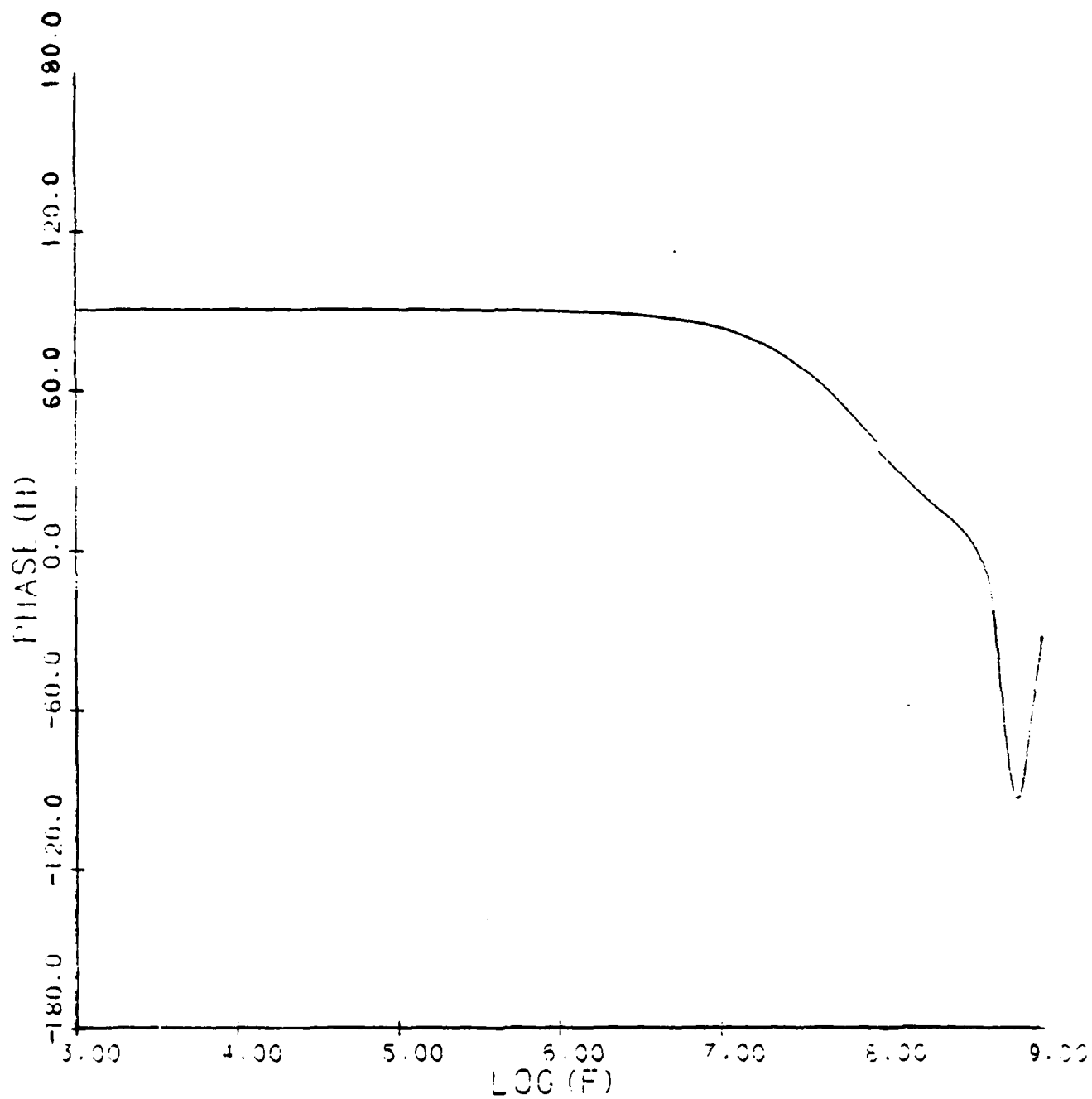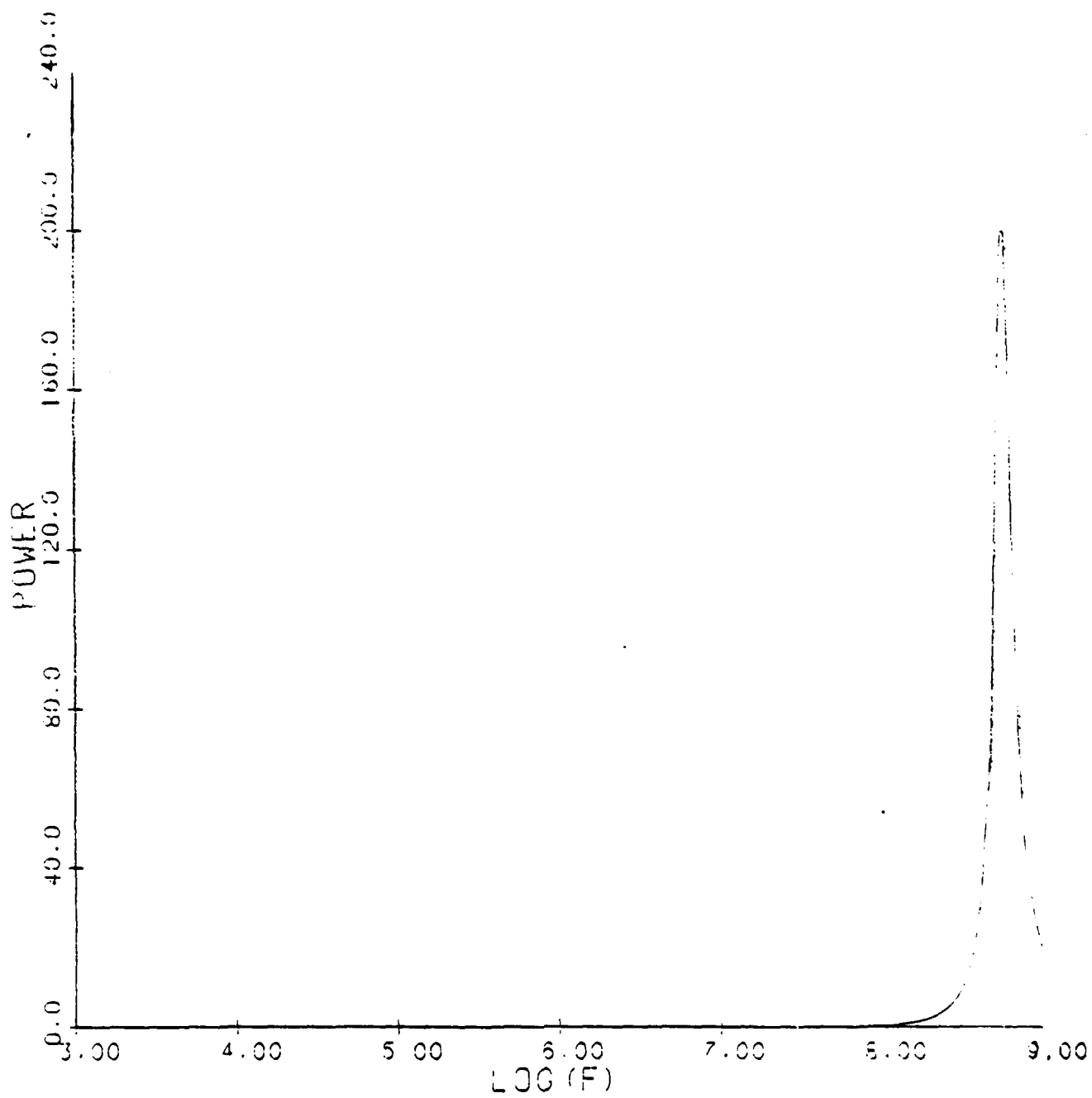
21

Figure 4.   b)   Phase

Figure 4.   c)   Scattered power
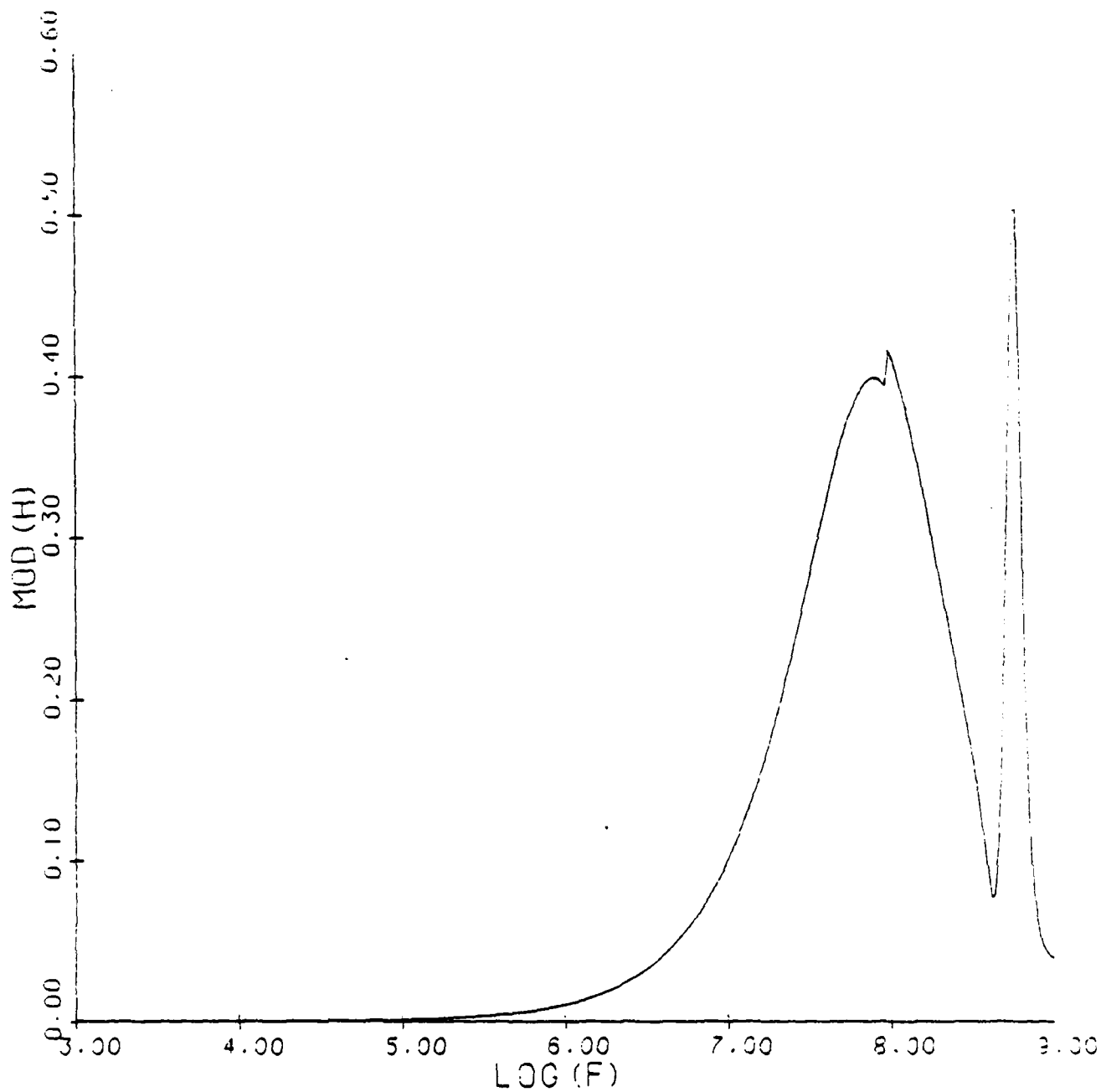
23

Figure 5. Second order transfer function $H_2(f_1, f_2)$ and contribution to scattered power with $f_1 = 20$ KHz. a) magnitude.
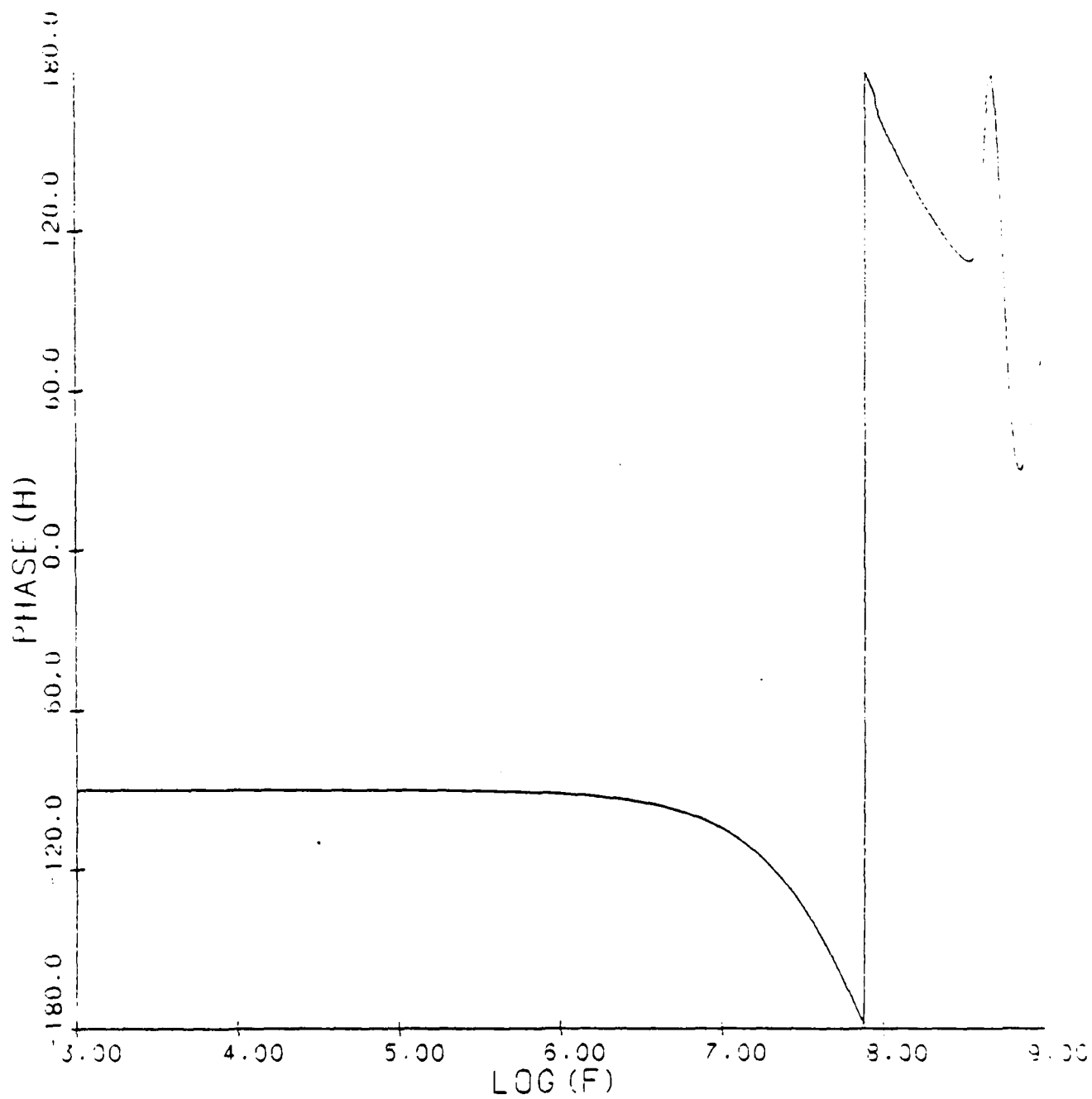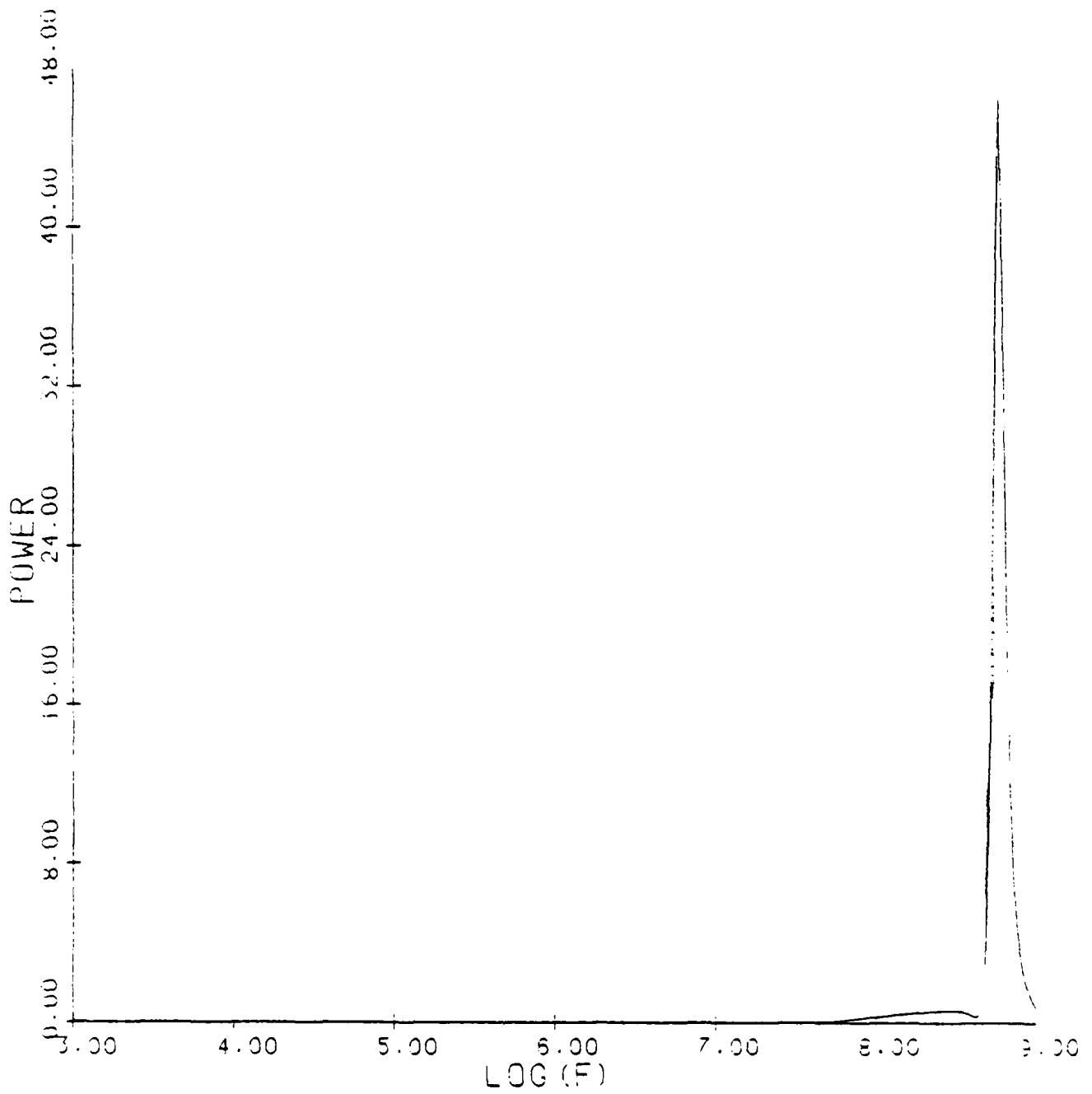
24

Figure 5.   b) Phase

25

Figure 5.   c)   Scattered Power.

the second order response only. The representation of the
power is also a bit confusing: the second order power is also
a function of 2 frequencies, one of which is fixed at 20 KHz.
However, the power is radiated at the frequency 20 KHz + $w/2\pi$.
The discontinuity in the mod (H) plot at about 100 MHz is due
to the transition from the short dipole model to the
Schelkunoff method of calcullating antenna impedance: it is an
artifact and is unimportant. The maximum in radiated power
occurs at approximately 575 MHz. The magnitude of the second
order transfer function has 2 maxima, one at about 100 MHz,
and the other at about 560 MHz.

Lastly, we present the third order transfer function
$H_3(w_1, w_2, w_3)$. In Figure 6, w_1 and w_2 are both fixed at 20 KHz.
The power in the figure is radiated at frequency $w/2\pi + 40$
KHz. There are 2 maxima in magnitude of H_3, at about 100 MHz
and 575 MHz, while the maximum power is radiated at 575 MHz.
Note the similarity in the shape of these curves and those of
Figure 5.

A more practical representation of the data is by the
frequency terms in the solution $v_o(t)=v_1(t)+v_2(t)+v_3(t)$ where
these are given by (15). To do this, we need to specify the
source term $g(t) = i_{sc}(t) + v(t)/R_L$ The short circuit antenna
current is due to a single plane wave incident broadside so
that at the antenna, the incident plane wave is

$E_o \cos(w_o t)$

This produces Fourier coefficients

$$g_i = \frac{1}{2} \frac{L_{eff}(w_i) E_o}{Z(w_i)} \qquad\qquad i = 1,2 \qquad\qquad (25)$$

where $w_1 = w_o$, $w_2 = -w_o$. Similarly, the circuit voltage source
is also a single sinusoid:

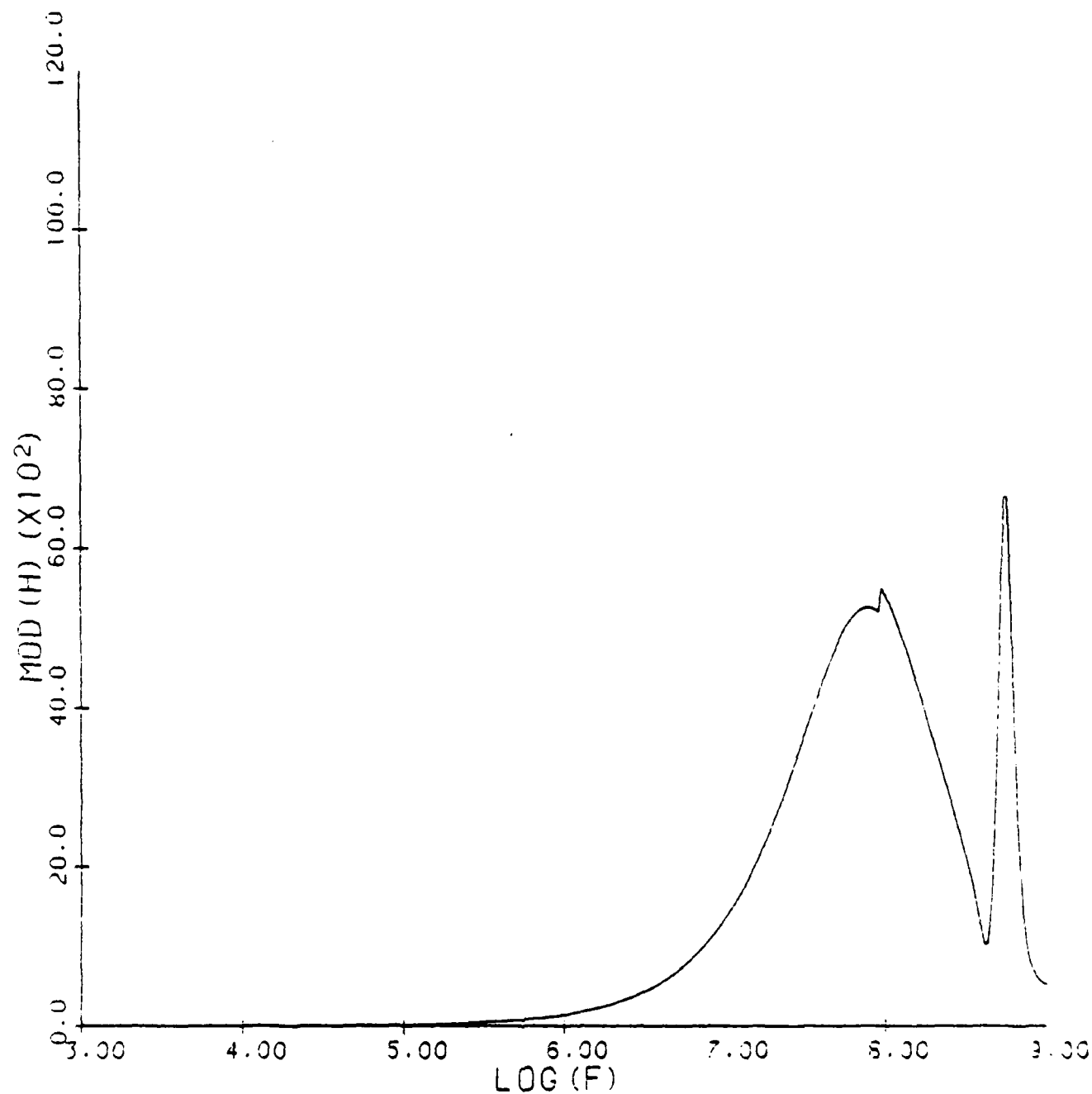$v(t) = v_c \cos(w_c t)$

27

Figure 6.   Third order transfer function $H_3(f_1, f_2, f_3)$ and
contribution to scattered power with $f_1 = f_2 =$
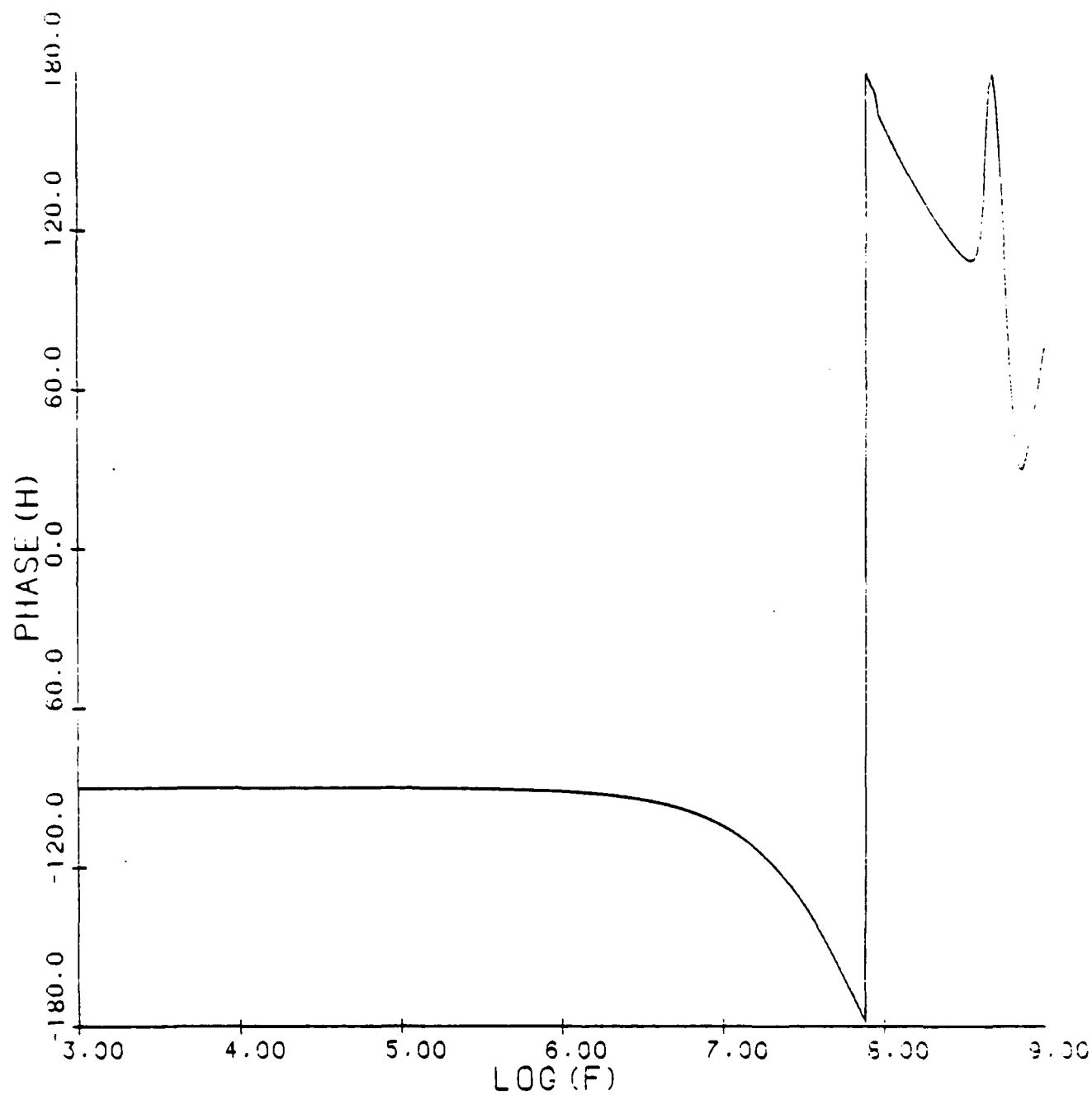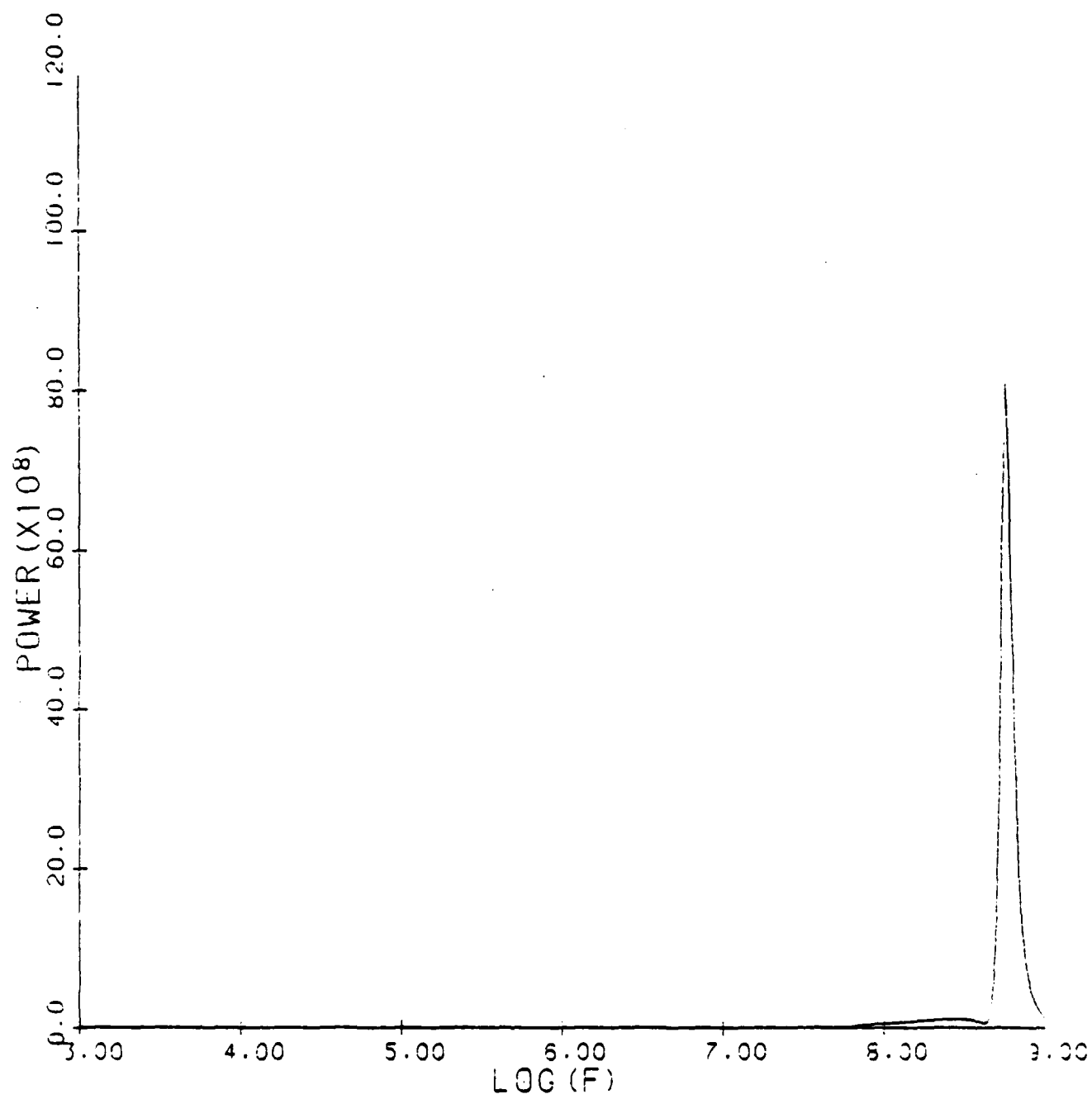20 KHz.   a)   Magnitude.

28

Figure 6.   b)   Phase

29

Figure 6.   c)   Scattered Power.

which produces Fourier components of $g(t)$

$$g_i = V_c/2R_L \qquad (26)$$

where $i = 3, 4$, and $w_2 = w_c$, $w_4 = -w_c$.

Thus, the Fourier series for $g(t)$ has 4 contributions and is given by:

$$g(t) = \frac{1}{2} \frac{L_{eff}(w_0)E_0}{Z(w_0)}e^{jw_0t} + \frac{1}{2} \frac{L_{eff}(w_0)E_0}{Z(w_0)}e^{jw_0t} + \frac{V_c}{2R_L}e^{jw_ct} + \frac{V_c}{2R_L}e^{jw_ct} \qquad (27)$$

If we set the circuit voltage frequency w_c to 20 KHz, an audio frequency, and the incident plane wave frequency to 500 MHz, an RF frequency, the Volterra series solution will produce frequency terms that are represented schematically in Figure 7. Note that some of the terms are simply the second and third harmonies. The more interesting terms are the mixtures of w_c and w_0. Because $w_0 \gg w_c$, the nonlinearity results in the appearance of sidebands about w_0 and $2w_0$. The pattern that emerges should be apparent: if we were to carry the Volterra series to fourth order, more sidebands would appear about w_0, $2w_0$ and they would emerge about $3w_0$. The usefulness of these sidebands stems from the antenna response. Although the antenna radiates negligibly at 20 KHz, it radiates strongly in the vicinity of 500 MHz and 1 GHz. Thus, the nonlinearity results in the incident RF plane wave being scattered as, in effect, a carrier wave for the 20 KHz signal in the circuit.

In Table 1, we show the results of our simulation with unit applied voltage (i.e., 1 volt) at 20 KHz and with a unit incident plane wave (i.e., 1 volt/m) at 500 MHz. The table lists the Fourier components of the solution at only positive frequencies; the total solution for the voltage across the

31
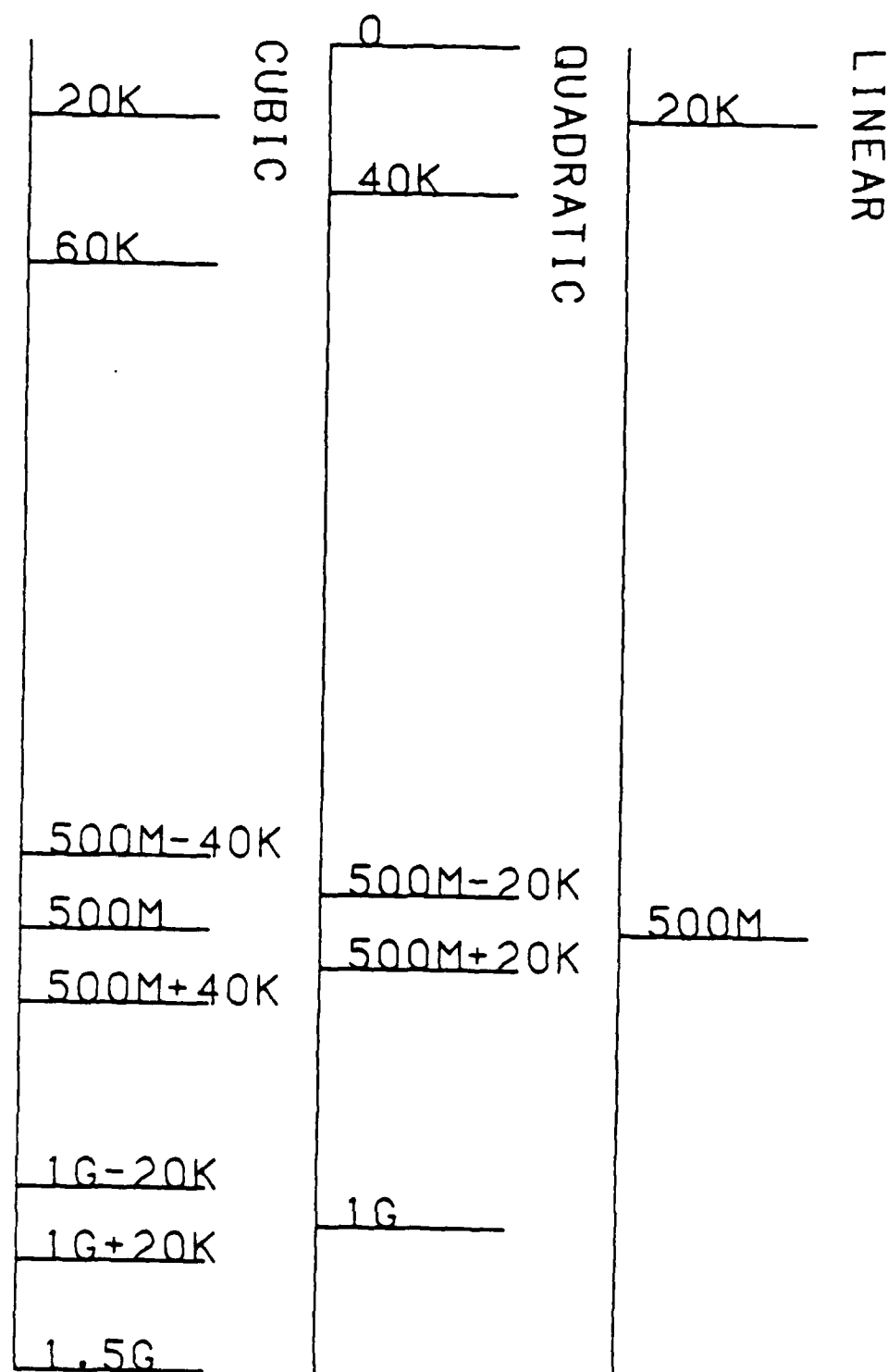
Figure 7. Line Spectrum of Volterra series terms for input frequencies of 20KHz and 500MHz.

f(Hz)	mod (v_d) (volts)	arg (v_d)	scattered power (watts)
linear			
20K	.5	0	3.8×10^{-22}
500M	.12	153.	7.3×10^{-5}
quadratic			
40K	3.9×10^{-4}	180.	3.7×10^{-27}
1G	3.0×10^{5}	51.	8.7×10^{-15}
0	7.8×10^{4}	180	0
500M$\pm$20K	2.9×10^{5}	-9.4	4.4×10^{-12}
cubic			
60K	2.6×10^{-3}	180.	8.2×10^{-24}
1.5G	4.6×10^{-6}	-142.	5.9×10^{-14}
500M	5.8×10^{-4}	-9.4	1.7×10^{-9}
20K	7.7×10^{-3}	180.	9.1×10^{-26}
500M$\pm$40K	2.9×10^{-4}	-9.4	4.3×10^{-10}
1G$\pm$20K	5.8×10^{-5}	51.	3.4×10^{-12}

Table 1: Frequency components of simulation of Volterra series solution. Circuit voltage source is 1 volt at 20 KHz, while the incident plane wave is 1 volt/m at 500 MHz.

diode is constructed as the sum of negative and positive frequency terms of equal amplitude, thus producing terms with a time dependence of the form $\cos(wt+\phi)$. Our focus here will be on the scattered or radiated power. The largest scattered power is due to the simple linear scattering of the incident plane wave. Note that the cubic nonlinearity produces correction terms at both 500 M and 20 K that serve to reduce the magnitude of the linear response at these frequencies: this is the compression term (Graham & Ehrman, 1973), a well known linear effect. Indeed, all nonlinear terms of odd order will contribute responses at the fundamental frequencies. For our purposes, the components of most interest are the intermodulation or mixture components at 500 M $\pm$ 20 K, 1 G $\pm$ 20 K and 500 M $\pm$ 40 K. As can be seen from the table, the largest radiated power occurs at 500 MHz and the side bands of $\pm$ 20 KHz and $\pm$ 40 KHz. Since this simulation is for unit input, we can construct the solution for these frequencies and voltage amplitude v_0 and plane wave amplitude E_0 by using the following simple proportionality relations. Since power depends on the square of current, we have (P_1 = power for unit input):

$$
\begin{aligned}
f &= 500 \text{ M} & P &= (E_0)^2 P_1 & (28)\\
f &= 500 \text{ M} \pm 20 \text{ K} & P &= (E_0 v_0)^2 P_1 \\
f &= 500 \text{ M} \pm 40 \text{ K} & P &= (E_0 v_0^2)^2 P_1 \\
f &= 1 \text{ G} \pm 20 \text{ K} & P &= (E_0 v_0)^2 P_1
\end{aligned}
$$

For example, if v_0 = 10 volts and E_0 = 1 volt, we get from (28) and Table 1:

$$
\begin{aligned}
f &= 500 \text{ M} & P &= 7.3 \times 10^5 \\
f &= 500 \text{ M} \pm 20 \text{ K} & P &= 4.4 \times 10^{10} \\
f &= 500 \text{ M} \pm 40 \text{ K} & P &= 4.3 \times 10^6 \\
f &= 1 \text{ G} \pm 20 \text{ K} & P &= 3.4 \times 10^{10}
\end{aligned}
$$

Note that the component at 500 M $\pm$ 40 K differs from the linear term by only a factor of 10.

We have previously seen that the scattered power due to the second and third order transfer functions is a maximum at 57 Hz for a circuit voltage of 20 KHz. We present the result of a simulation at these frequencies in Table 2. A comparison of the results of Tables 1 and 2 shows that the intermodulation components 575 M $\pm$ 20 K and 575 M $\pm$ 40 K are larger than those corresponding to the 500 M plane wave by about a factor of 2. This relatively small change is due to the relatively broadband nature of the antenna.

f(Hz)	mod (v_d) (volts)	arg (v_d)	scattered power (watts)
linear			
20K	.5	0	3.8×10^{-22}
575M	.125	111.	3.3×10^{-5}
quadratic			
40K	3.9×10^{-4}	180.	3.7×10^{-27}
1.15G	2.5×10^{-6}	-35.	6.7×10^{-15}
0	7.8×10^{-4}	180	0
575M±20K	6.0×10^{-5}	-86.	7.7×10^{-12}
cubic			
60K	2.6×10^{-3}	180.	1.9×10^{-14}
1.725G	3.6×10^{-6}	77.	8.2×10^{-25}
575M	1.2×10^{-2}	-86.	3.0×10^{-9}
20K	7.7×10^{-3}	180.	9.1×10^{-26}
575M±40K	5.9×10^{-4}	-86.	7.5×10^{-10}
1.15G±20K	4.9×10^{-4}	-35.	2.6×10^{-12}

Table 2: Frequency components of simulation of Volterra series solution. Circuit voltage source is 1 volt at 20 KHz while the incident plane wave is 1 volt/m at 575 MHz.

CONCLUSION:

The simulations we have performed have shown that an RF field is scattered by the active diode circuit in such a manner that the RF frequency acts as a carrier for the circuit signal. If the circuit has an applied sinusoid of 20 KHz, then, in the absence of any RF signal, the diode nonlinearity results in the voltage across the diode having Fourier components of 20 KHz, 40 KHz, and higher harmonics. With an RF plane wave of frequency w_o incident on the antenna, the resulting circuit current and scattered power has frequency components of $w_o \pm 20$ KHz, $w_o \pm 40$ KHz, etc. There are also components at $2w_o \pm 20$ KHz, $2w_o \pm 40$ KHz, etc. and the same is true for the higher harmonics of w_o. Thus, each harmonic of the RF signal acts as a carrier wave for the circuit signal, in the sense that the frequency composition of the circuit signal is shifted from being centered about zero to a center given by the harmonic. The relative magnitudes of the circuit signal are not exactly reproduced in the scattered waves at the RF frequency and its harmonics. It should be stated that although we have focused the discussion on the scattering by the circuit, there are also interference effects in the circuit due to the interaction of the circuit signal and the RF signal.

We have performed calculations of a few of these scattered intermodulation components using a Volterra series approach. Since this is a perturbation method, the numerical values derived can be regarded as providing reliable information only when our assumption of small voltage across the diode is appropriate, or more specifically, from (8), when the voltage is less than 0.026 volts. The data presented in the tables violate this assumption. However, by appropriate

scaling of the unit responses, numerical values could be easily generated which are consistent with the perturbation approximation. Nevertheless, the formalism and numerical values provide a semi-quantitative description for the case where the approximation does not hold. A further limitation of this modeling is suggested by Franceschetti and Pinto (1980). These authors claim that a model of the diode which ignores the nonlinear junction capacitive effects is justified only at frequencies less than 1 MHz. A more precise model would include these nonlinear capacitive effects and would carry out the Volterra series solution to a higher order. However, the computation of the transfer function for orders higher than five is extremely difficult and this situation limits the applicability of the Volterra series method to the mildly nonlinear case.

REFERENCES

Franceschetti, G. and Pinto, I., "Nonlinearly Loaded Antennas" in Nonlinear Electromagnetics, Uslenghi, P.L.E. ,ed., Academic Press, N.Y., 1980.

Graham, J.W. and Ehrman, L., eds., "Nonlinear Systems Modeling and Analysis with Applications to Communications Receivers", RADC-TR-73-178 Rome Air Development Center, Griffiss AFB, N.Y., 1973, AD 766278.

Jordan, E.C. and Balmain, K.G., Electromagnetic Waves and Radiating Systems, 2nd edition, Prentice-Hall, Englewood Cliffs, N.J., 1968.

Landt, J.A., Miller, E.K. and Deadrick, F.J., "Time Domain Modeling of Nonlinear Loads", IEEE Trans. Antennas Propagat., AP-31, p 121, 1983.

Liu, T.K. and Tesche, F.M., "Analysis of Antennas and Scatterers with Nonlinear Loads", IEEE Trans. Antennas Propagat., AP-24, p 131, 1976.

Kanda, M., "Analytical and Numerical Techniques for Analyzing an Electrically Short Dipole with a Nonlinear Load", IEEE Trans. Antennas Propagat., AP-28, p. 71, 1980.

Sarkar, T.K. and Weiner, D.D., "Scattering Analysis of Nonlinearly Loaded Antennas", IEEE Trans. Antennas Propagat., AP-24, p. 125, 1976.

Schetzen, M., The Volterra and Weiner Theories of Nonlinear
Systems, Wiley, N.Y., 1980.

Tai, C.T., "Characteristics of Linear Antenna Elements" in
Antenna Engineering Handbook, Jasik, H.,
ed., McGraw-Hill, N.Y., 1961.